

Critical exponents of the three-dimensional Ising universality class from finite-size scaling with standard and improved actions

M. Hasenbusch*

Fachbereich Physik, Humboldt-Universität zu Berlin, Invalidenstrasse 110, D-10115 Berlin, Germany

K. Pinn[†] and S. Vinti[‡]

Institut für Theoretische Physik I, Universität Münster, Wilhelm-Klemm-Strasse 9, D-48149 Münster, Germany

(Received 17 June 1998; revised manuscript received 19 January 1999)

We compute an improved action for the Ising universality class in three dimensions that has suppressed leading corrections to scaling. It is obtained by tuning models with two coupling constants. We studied three different models: the ± 1 Ising model with nearest-neighbor and body diagonal interaction, the spin-1 model with states $0, \pm 1$, and nearest-neighbor interaction, and ϕ^4 theory on the lattice (Landau-Ginzburg model). The remarkable finite-size scaling properties of the suitably tuned spin-1 model are compared in detail with those of the standard Ising model. Great care is taken to estimate the systematic errors from residual corrections to scaling. Our best estimates for the critical exponents are $\nu=0.6298(5)$ and $\eta=0.0366(8)$, where the given error estimates take into account the statistical and systematic uncertainties. [S0163-1829(99)06317-1]

I. INTRODUCTION

In Monte Carlo simulations the system size is limited by the memory of the computer and by the available CPU time. Therefore, in many instances, finite-size scaling² is the key to a precise determination of properties of statistical systems at criticality. Finite-size scaling laws are affected by corrections to scaling. These corrections cause systematic errors in the results for universal quantities one is interested in. With improving statistical accuracy of the Monte Carlo data it becomes important to deal properly with systematic errors. One way to proceed is to include corrections to scaling into the fit *Ansätze* when analyzing the data. Another, more fundamental way is to remove corrections already from the system to be studied.

Renormalization group³ (RG) offers (at least in principle) a way to achieve this goal. RG fixed points are free of corrections to scaling. Such actions, however, contain in general an infinite number of couplings. In practical applications one is forced to truncate the action to a finite number of terms, which in fact is an uncontrolled approximation. For an application of this strategy to asymptotically free models see the work on perfect actions.⁴ Note that we follow Euclidean field theory convention. In statistical mechanics language one would say Hamiltonian instead of action.

A different approach was pioneered by Symanzik.⁵ Higher order terms are added to the action. By imposing certain conditions on observables leading corrections to scaling are eliminated. While Symanzik formulated his method in the framework of perturbation theory, recently there have been attempts to apply this method in a nonperturbative, i.e., numerical, setting.⁶

Our present approach is closer to this latter point of view than to the block-spin renormalization-group-inspired framework. The idea is to improve the scaling properties of Ising models by moving to models with generalized actions and tuning the coupling constants as to obtain reduced corrections to scaling.

The removal of leading corrections to scaling (though not in the context of finite-size scaling) was first proposed and investigated by Fisher and co-workers.⁷ Reduction of corrections to finite-size scaling was investigated by Blöte *et al.*,⁸ however, without a clear description of the principle and method used to obtain the improved scaling properties.

In the present work, we are able to reduce the corrections to scaling in various quantities dramatically. This is achieved by tuning the two coupling constants of a generalized Ising model in the proper way. Especially the Binder cumulant and its derivatives, and also the susceptibility, can be fitted to scaling laws without corrections to scaling terms, yielding very precise estimates of the three-dimensional (3D) Ising critical exponents.

It was argued in Refs. 9 and 10 that the improvement mentioned above does not lead to reduced error estimates for critical exponents. The authors claimed that our error estimates are underestimated, since we do not take into account residual leading corrections to scaling. Such corrections might well be present, because the parameters of our improved model are computed numerically. However, this is not the full story as we shall explain in this paper. Our argument is based on the fact that ratios of correction to scaling amplitudes are universal.

In this paper, we describe in detail our method, the numerical results, and the fitting procedures. We confront the results from the improved action with high-precision data from simulations of the standard Ising model, estimating with a well-defined procedure systematic errors for both actions.

The interested reader can access a more detailed version of this paper (including further tables of Monte Carlo and fit results) in the internet.¹

II. IMPROVING THE SCALING BEHAVIOR

A. The models

Usually, Monte Carlo studies of the Ising model are done using what in field theory is called standard action,

$$S = -\beta \sum_{\langle i,j \rangle} s_i s_j. \quad (1)$$

The s_i take values ± 1 , and the spin-spin interaction is a sum over all nearest-neighbor pairs $\langle i,j \rangle$. A precise estimate for the critical coupling was obtained in Ref. 11: $\beta_c = 0.221\,654\,4(3)(3)$.

In the following, we will introduce and study three different models in the 3D Ising universality class, each of them governed by *two* coupling constants. In all three cases the Boltzmann factor is given by $\exp(-S)$.

Spin-1 model

$$S = -\beta \sum_{\langle i,j \rangle} s_i s_j + D \sum_i s_i^2. \quad (2)$$

The s_i take values $0, \pm 1$, and the spin-spin interaction is a sum over all nearest-neighbor pairs. This model was considered in Ref. 8. There, D was fixed to $\ln 2$. The critical β corresponding to this particular value of D was estimated in Ref. 8 to be $\beta_c = 0.393\,422\,4(10)$.

Next-nearest neighbor (NNN) model

$$S = -\beta_1 \sum_{\langle i,j \rangle} s_i s_j - \beta_2 \sum_{[i,j]} s_i s_j. \quad (3)$$

The s_i take values ± 1 , and the spin-spin interaction is a sum over all nearest-neighbor pairs $\langle i,j \rangle$ and third-neighbor pairs (body diagonals) $[i,j]$. Blöte *et al.* fixed $\beta_2/\beta_1 = 0.4$ and obtained $\beta_{1,c} = 0.128\,003\,6(5)$.

ϕ^4 model

$$S = -\beta \sum_{\langle i,j \rangle} \phi_i \phi_j + \sum_i \phi_i^2 + \lambda \sum_i (\phi_i^2 - 1)^2. \quad (4)$$

The variables ϕ assume real values. In the limit $\lambda \rightarrow \infty$ one recovers the standard Ising model.

The three two-coupling models have a second-order critical line in the space spanned by the two coupling constants. We shall exploit the degree of freedom of moving on the critical line to find models with reduced corrections to scaling.

B. Matching of phenomenological couplings

We study two independent phenomenological couplings of the 3D Ising model, to be called R_i , $i=1,2$ in the following. Both quantities are universal, i.e., at criticality their infinite volume limit R_i^* does not depend on details of the action. R_1 is the ratio of partition functions with antiperiodic and periodic boundary conditions, respectively,

$$R_1 = Z_a/Z_p. \quad (5)$$

The lattices will always be cubical, with extension L in each of the three directions. Antiperiodic boundary conditions are imposed only in one of the three lattice directions. R_2 is the Binder cumulant,

$$R_2 = Q = \frac{\langle m^2 \rangle^2}{\langle m^4 \rangle}. \quad (6)$$

Here, m denotes the magnetization per spin,

$$m = L^{-3} \sum_i s_i. \quad (7)$$

The R_i are L dependent and, of course, functions of the coupling parameters in the action. For the two-coupling models defined above, we define ‘‘flows’’ (lines of constant physics) $(K_1(L), K_2(L))$ by requiring that

$$R_i(L, K_1(L), K_2(L)) = R_i^*. \quad (8)$$

K_1 and K_2 represent the two coupling constants of the model. In the next subsection we shall demonstrate that with increasing L the flows of (K_1, K_2) converge towards a critical point that has no leading order corrections to scaling.

C. RG analysis of the matching condition

The main features of the two-coupling models can be discussed in the framework of the renormalization group. The scaling properties can be derived from the linearized RG transformation at the fixed point.

We consider general actions with couplings K_α , where $\alpha=1,2,\dots$. An RG transformation, realized, e.g., by a block-spin transformation, changes these couplings according to $K \rightarrow K'(K) = R(K)$. A fixed point K^* is defined through $R(K^*) = K^*$. The linearized transformation at the fixed point can be represented by a matrix

$$T_{\alpha\beta} = \left. \frac{\partial K'_\alpha}{\partial K_\beta} \right|_{K=K^*}. \quad (9)$$

One introduces ‘‘normal coordinates’’ (scaling fields) by

$$u_i = u_i(K) = \sum_\alpha \varphi_{i,\alpha} (K_\alpha - K_\alpha^*), \quad (10)$$

where φ_i denotes the i th (left) eigenvector of the matrix T ,

$$\sum_\alpha \varphi_{i,\alpha} T_{\alpha\beta} = \lambda_i \varphi_{i,\beta}. \quad (11)$$

The u_i transform under RG transformations like $u_i \rightarrow \lambda_i u_i$. In Ising-type models the leading eigenvalues are given by

$$\lambda_1 = b^{1/\nu}, \quad \lambda_2 = b^{-\omega}, \quad \lambda_3 = b^{-x}, \quad (12)$$

where $x \gg \omega$. Note that $x=2$ for the Gaussian model. From leading order ϵ expansion one expects that x is close to 2 at the Wilson-Fisher fixed point. b denotes the scale factor of the RG transformation.

We now assume that we have only two nonvanishing couplings K_1 and K_2 in our action. Let us then write down explicitly the condition for being critical ($u_1=0$) and eliminating the leading corrections to scaling ($u_2=0$). The first condition reads

$$\varphi_{1,1}(K_1 - K_1^*) + \varphi_{1,2}(K_2 - K_2^*) = \kappa_{1,3}, \quad (13)$$

whereas the condition $u_2=0$ translates to

$$\varphi_{2,1}(K_1 - K_1^*) + \varphi_{2,2}(K_2 - K_2^*) = \kappa_{2,3}. \quad (14)$$

For $i=1,2$, the $\kappa_{i,3}$ are given by

$$\kappa_{i,3} = \sum_{\alpha \geq 3} \varphi_{i,\alpha} K_\alpha^*. \quad (15)$$

Let us now study how our matching procedure with the two quantities $R_1 = Z_a/Z_p$ and $R_2 = Q$ works. The R_k are functions of the bare couplings and the lattice size

$$R_k = R_k(L, K_1, K_2). \quad (16)$$

We express these quantities as functions of the scaling fields defined above,

$$R_k(L, K_1, K_2) = R_k(L^{1/\nu} u_1^{(1)}, L^{-\omega} u_2^{(1)}). \quad (17)$$

Here, the upper index ⁽¹⁾ indicates that the scaling field is taken at the scale of the lattice spacing. The prefactor promotes the scaling field to its value at the scale L . Taylor expansion of the R_k around their fixed point values yields

$$R_k \approx R_k^* + r_{k,1} L^{1/\nu} u_1^{(1)} + r_{k,2} L^{-\omega} u_2^{(1)}. \quad (18)$$

The matching conditions $R_k = R_k^*$ are thus equivalent to

$$r_{k,1} L^{1/\nu} u_1^{(1)} + r_{k,2} L^{-\omega} u_2^{(1)} = 0, \quad (19)$$

for $k=1,2$. We obtain, as desired, the solution $u_1^{(1)} = 0$ (criticality) and $u_2^{(1)} = 0$ (no leading order corrections). Including higher order corrections in the scaling *ansatz*, governed by u_3 and exponent λ_3 , one can convince oneself that fixing R_1 and R_2 to their fixed point values leads to convergence to the critical line $u_1 = 0$ with corrections that decay like $L^{-x-1/\nu}$. The $u_2 = 0$ condition is approached with a much slower rate, namely like $L^{-x+\omega}$.

D. Computing the matching flows

For the three two-coupling models specified above, we set up a procedure to determine the flows of couplings $(K_1(L), K_2(L))$ such that Eq. (8) was fulfilled. To this end, we used estimates for $R_1^* = 0.5425(10)$ and $R_2^* = 0.6240(10)$, which were an outcome of a preliminary analysis of data obtained using the standard action, cf. Sec. IV B.

The matching couplings were searched for using a Newton iteration, based on the inversion of a matrix made up from Monte Carlo estimates of the derivatives of the R_i with respect to the two couplings. Typically, three to four iterations were sufficient to find couplings such that Z_a/Z_p and Q attained the prescribed values within the given statistical precision. The results are given in Table I.

A first look at the table reveals that both for the spin 1 and the ϕ^4 model, the flow converges to a fixed point quickly, whereas it keeps moving strongly in the case of the NNN model. A rough explanation of this could be the following: In order to remove the leading corrections to scaling, one has to move efficiently between the Gaussian model (equivalent to the ϕ^4 model with vanishing λ) and the Wilson-Fisher fixed point. Moving between these two fixed points is most efficiently done using a ϕ^4 -type coupling, which is implicitly present also in the spin-1 model. The NNN model seems to

TABLE I. Flows of couplings defined such that for all lattice sizes the two quantities $R_1 = Z_a/Z_p$ and $R_2 = Q$ match (to the given statistical precision) with their fixed point values $R_1^* = 0.5425(10)$ and $R_2^* = 0.6240(10)$.

Spin-1 model				
L	β	D	Z_a/Z_p	Q
3	0.35737	0.4401	0.54201(30)	0.62447(21)
4	0.37250	0.5510	0.54242(25)	0.62347(18)
5	0.37794	0.5883	0.54292(19)	0.62421(15)
6	0.38210	0.6169	0.54221(49)	0.62426(35)
7	0.38419	0.6311	0.54326(30)	0.62366(22)
8	0.38320	0.6241	0.54291(37)	0.62430(27)
9	0.38320	0.6241	0.54259(60)	0.62403(44)
10	0.38320	0.6241	0.54288(57)	0.62431(42)
NNN model				
L	β_1	β_2	Z_a/Z_p	Q
4	0.12266	0.05406	0.5429(2)	0.6238(2)
5	0.12928	0.05028	0.5427(1)	0.6241(2)
6	0.13431	0.04734	0.5425(1)	0.62441(8)
7	0.13800	0.04518	0.5425(3)	0.6242(2)
8	0.14069	0.04361	0.5426(2)	0.6243(1)
9	0.14292	0.04231	0.5430(2)	0.6232(1)
10	0.14406	0.04165	0.5425(2)	0.6242(2)
11	0.14590	0.04059	0.5429(1)	0.62385(8)
12	0.14724	0.03981	0.5426(1)	0.6235(1)
13	0.14808	0.03933	0.5431(1)	0.6236(1)
ϕ^4 model				
L	β	λ	Z_a/Z_p	Q
3	0.35303	1.5248	0.5420(3)	0.6244(2)
4	0.36338	1.3282	0.5425(3)	0.6243(2)
5	0.36908	1.2188	0.5425(2)	0.6241(1)
6	0.37165	1.1689	0.5427(2)	0.6241(1)
7	0.37270	1.1481	0.5424(2)	0.6243(1)
8	0.37308	1.1410	0.5421(1)	0.6245(1)
9	0.37273	1.1479	0.5416(3)	0.6247(2)

need renormalization to a larger scale in order to come close to the flow line connecting the Gaussian with the Wilson-Fisher fixed point.

Plotting the second coupling vs the first one, one finds that with very good precision the critical line can be approximated by a straight line

$$K_2(L) = a_1 + a_2 K_1(L), \quad (20)$$

with $a_1 = -2.04, 0.1253, 8.29$, and $a_2 = -6.95, -0.5804, -19.17$ for the spin-1, the NNN and the ϕ^4 model, respectively. For the spin 1 and the NNN model, our estimates for the critical lines can be compared with results by Blöte *et al.* They are in good agreement. Fits of $K_1(L)$ with a power law $K_1(L) = c_1 + c_2 L^{-\alpha}$ yielded good fits in all cases, with exponents of order 3 in the cases of spin-1 and ϕ^4 models. Note that this exponent is much larger than $x - \omega$, which is expected to be around 1. A possible explanation for this is that the amplitudes in front of the correction term with an expo-

ment $x \approx 2$ are of negligible size, while corrections with an exponent $x \approx 4$ have a very large amplitude. For the NNN model, α is of order 1.

The slow convergence of the NNN flow motivated our decision to discard this model from further investigation. The behavior of the ϕ^4 and spin-1 models appears to be very similar. Since the spin-1 model is faster to simulate than the ϕ^4 model we concentrate in the following on the spin-1 model, and leave the ϕ^4 model for later study.

Note that our result for the optimal $\lambda \approx 1.145$ of the ϕ^4 model is consistent with the observation in Ref. 10 that the optimal λ should be close to one.

E. Identification of the $u_2=0$ line

Next, we determined an approximation of the $u_2=0$ manifold. This was done by looking at the derivatives of the R_i at criticality. From the RG analysis of Sec. II C one infers

$$\frac{\partial R_k}{\partial K_\alpha} = \sum_i \frac{\partial R_k}{\partial u_i} \frac{\partial u_i}{\partial K_\alpha} = r_{k,1} L^{1/\nu} \varphi_{1,\alpha} + r_{k,2} L^{-\omega} \varphi_{2,\alpha}. \quad (21)$$

The left-hand side of the equation can be determined by Monte Carlo simulation and will therefore be assumed as known. Taking into account that without loss of generality one can set $\varphi_{i,1} \equiv 1$, the equations can be solved (or fitted) if the left-hand side is known at least for two different lattice sizes. We performed Monte Carlo simulations at $(\beta, D) = (0.3832, 0.6241)$ for lattice sizes 10, 12, 16, 20, and 32. Fixing the exponents $\nu=0.63$ and $\omega=0.81$ (Ref. 12) we obtained that the scaling field $\phi_{2,2}$ should be approximately $-1/3$. This result is quite stable under small variations of the fixed parameters ν and ω .

Plugging this into Eq. (14), one obtains that $3\beta-D$ should be kept constant. We used our simulation point $(0.3832, 0.6241)$ to fix this constant. In conclusion, one should approach criticality by varying β while adjusting D according to

$$D = 3(\beta - 0.3832) + 0.6241. \quad (22)$$

Of course, a precise estimate of β_c along this line still has to be determined. This will be discussed in the next section.

The fit result for $\varphi_{1,2}$ can be used to perform a consistency check. Ignoring higher couplings, one should have $(\beta - \beta^*) + \varphi_{1,2}(D - D^*) = 0$. Solving for D and plugging in the values $\beta^* = 0.3832$, $D^* = 0.6241$, and $\varphi_{1,2} = -0.1439$ one obtains with good precision the critical-line approximation $D = -2.04 + 6.95\beta$. We remark that errors in the precise estimation of the $u_2=0$ line affect results for the critical exponents only weakly. E.g., the effect on the exponent ν is of order $L^{-1/\nu-\omega}$.

III. SIMULATION PARAMETERS AND STATISTICS

A. Standard action

Monte Carlo simulations of the 3D Ising model with standard action were performed at $\beta = 0.2216545$, which is a good approximation of the critical coupling.^{8,11}

For cubical lattices of size $L = 2, 3, 4, \dots, 19$ we performed simulations with the multispin demon update.^{13,14} The number of measurements ranges from 6.4×10^9 for $L=2$ to 1.4

$\times 10^9$ for $L=19$. The update algorithm is local. Hence one expects a dynamical critical exponent $z \approx 2$. However, due to the multispin coding implementation a single sweep can be done substantially faster than with the cluster algorithm. Therefore, one expects a better performance for the demon update on such small lattices.

For a subset of the smaller lattices, and for bigger lattices up to size 128, cluster update was performed, using a new variant of the algorithm, the *wall-cluster algorithm*. Note that there is quite a lot of freedom in the selection of clusters, which are flipped during one update step. In the wall-cluster algorithm, one flips all clusters that intersect with a given lattice plane. Sequentially one takes lattice planes in 1–2, 1–3, and 2–3 direction. The position is chosen randomly. Let us call the procedure to generate and flip all the clusters connected to the selected plane a wall-cluster update step. The motivation for choosing this type of update was that the construction of all clusters that have elements in a lattice plane is needed for the measurement of Z_a/Z_p anyway.

In order to test the performance of the new algorithm we performed runs on lattices of size $L=6$ up to $L=96$ with at least 300 000 measurements for each lattice size. The average sum of the sizes of the clusters per volume that are flipped in one step behaves as $S/V = CL^x$. Fitting our data to this law, discarding the results from $L < 24$, yields $S/V = 1.008(4)L^{-0.527(1)}$ ($\chi^2/\text{dof} = 0.4$). The integrated autocorrelation times of the energy, the susceptibility, and of the Z_a/Z_p measurements (see below) were also fitted to power laws, $\tau = cL^z$, using data from all lattice sizes. Only for τ_b the $L=6$ data were discarded. The results are $c = 1.04(2)$, $1.30(3)$, $0.60(2)$, and $z = 0.035(7)$, $-0.044(7)$, $-0.028(8)$ for the energy, the magnetic susceptibility, and the boundary variable, respectively.

These numbers should be compared with the corresponding ones from the single-cluster algorithm.¹⁵ Here the integrated autocorrelation times increase from $\tau = 1.36(2)$ to $\tau = 1.97(5)$ for the energy and from $\tau = 1.01(2)$ to $\tau = 1.20(3)$ for the magnetic susceptibility when the lattice size is increased from $L=16$ to $L=64$. These τ 's are fitted by $\tau_E \propto L^{0.28(2)}$ and $\tau_\chi \propto L^{0.14(2)}$.

Note that we obtain for the wall cluster $\tau = 1.17(2)$ for $L=16$ and $\tau = 1.26(2)$ for $L=64$ for the energy and $\tau = 1.19(2)$ for $L=16$ and $\tau = 1.10(2)$ for $L=64$ for the magnetic susceptibility.

We conclude that the exponents z of the wall-cluster algorithm are smaller than those of the single-cluster algorithm. For the lattice sizes in question, however, the actual τ 's are of similar size.

For the measurements of Z_a/Z_p we employed a variant of the boundary flip algorithm,¹⁶ where the cluster is not flipped but instead used to construct an observable.

We simulated the lattice sizes $L = 4, 6, 8, 10, 12, 14, 16, 20, 24, 28, 32, 40, 48, 56, 64, 80, 96, 112, \text{ and } 128$. The number of measurements ranges from 3×10^9 for $L=4$ to 6×10^5 for $L=128$. The total CPU consumption of the standard action runs was about 1.1 years on a 200 MHz Pentium Pro PC for the wall-cluster simulations. All simulations with the demon algorithm for the standard Ising model took about half a year on a 200 MHz Pentium Pro PC.

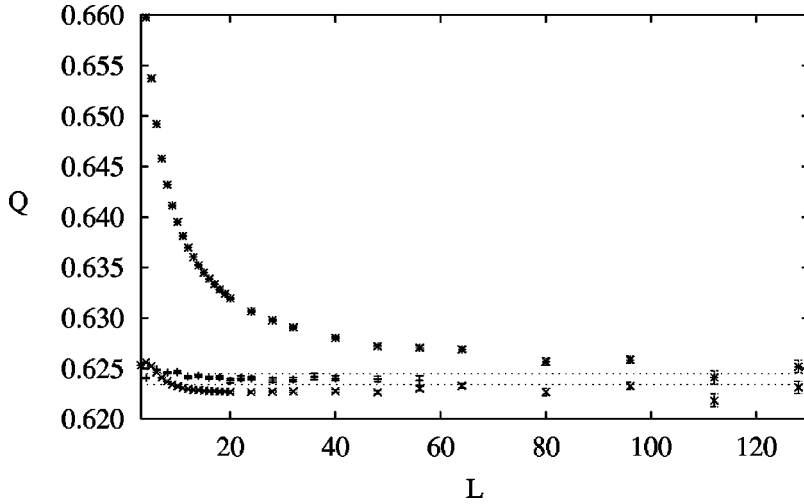


FIG. 1. $R_2=Q$ as function of lattice size for both models. The upper data (stars) are from the standard action. The bars (flat data) belong to the improved action. Crosses are used to show standard action results corrected with the leading correction to scaling contribution. The final estimate obtained from the fit analysis is plotted by dotted lines.

B. Improved action

A first estimate for β_c was obtained by locating the crossings of $R_i(L)$ with $R_i(2L)$. We used lattices of size $L=4,8,16,32$ and obtained $\beta_c=0.383\,245(10)$, with D given by Eq. (22), i.e., $D_c=0.624\,235$. Note that this was still a preliminary estimate to be refined later.

Monte Carlo simulations were then performed at $\beta=0.383\,245$, fixing D according to Eq. (22). We simulated on cubic lattices with linear extension L ranging from 4 to 56, using the single-cluster algorithm in alternation with a Metropolis procedure to maintain ergodicity. Two measurements were separated by three single-cluster updates and one Metropolis sweep. As for the standard action we used clusters built with the boundary flip algorithm to obtain estimates for Z_a/Z_p . After each growth of the corresponding cluster, the work done was also exploited to perform one wall-cluster step as described for the standard action above. The number of measurements ranges from 6×10^7 for $L=6$ to 2×10^6 for $L=56$. The runs for the determination of β_c took about three months of CPU on Pentium 166-MMX PCs, while the final production runs consumed a total of one year CPU on the same type of PC.

IV. ANALYZING THE DATA

Our aim is to test the improvement which can be reached in the estimates for the phenomenological couplings R_i and the critical exponents using the improved spin-1 action instead of the standard action.

We shall present results obtained from fitting our data to various finite-size scaling laws. It will turn out that the estimates obtained from the standard action are always compatible with those extracted from the improved action.

To give a first impression of the degree of improvement we plot various quantities as a function of L for the two actions. In Fig. 1, the Binder cumulants Q are plotted for the two actions, while in Fig. 2 the critical ratios Z_a/Z_p are given. In both figures, the final values obtained from our fit analysis are also given, together with error lines indicating the range of the estimated statistical plus the systematic error. Clearly the improved samples are much more stable and reach their asymptotic regime for very small lattice sizes, while the standard samples hardly get there on lattice sizes of

order 10^2 . In Fig. 1 we have in addition plotted the standard action result with the contribution of the leading order correction to scaling subtracted, namely $Q-0.105L^{-0.81}$.

The improved action data outperform the corrected standard action data. This is due to the fact that our improvement procedure not only eliminates correction terms of the form $L^{-\omega}$, but also higher order corrections of the form $L^{-n\omega}$, n integer, which are generated by the same scaling field. In particular, corrections of the type $L^{-2\omega}$ should be present in the observables of the standard Ising model. Interestingly, such corrections have not been taken into account, e.g., in the analysis by Blöte *et al.*,⁸ in spite of the fact that 2ω is smaller than other exponents taken into account in the fit *Ansätze*.

Because of their importance in extracting the critical exponents ν and η , we plot also the derivatives of Q and the susceptibilities χ , see Fig. 3. In order to check for a residual L dependence and to be able to compare the samples of the two models, the data have been rescaled. The Q derivatives have been multiplied by a factor $L^{-1/0.63}$ and normalized to their value at $L=56$ and $L=128$ for the improved and the standard action, respectively. Anticipating some results which will be presented below, the χ 's have been transformed by $\chi \rightarrow (\chi - c)L^{\eta-2}d^{-1}$, where c , η , and d are fit parameters.

The authors of Refs. 9 and 10 claim that the apparent

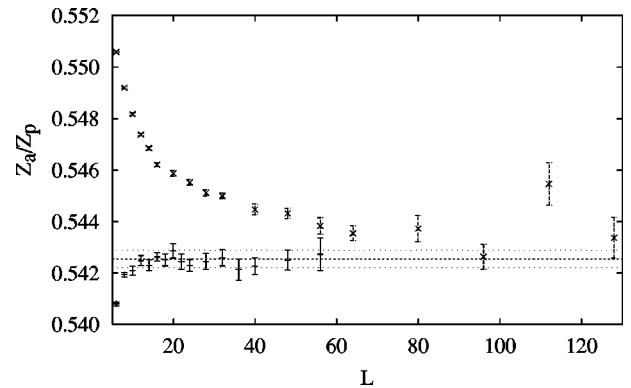


FIG. 2. $R_1=Z_a/Z_p$ as function of lattice size for both models. Standard action: crosses, improved action: bars. The final estimate obtained from our fit analysis is also plotted with an error interval.

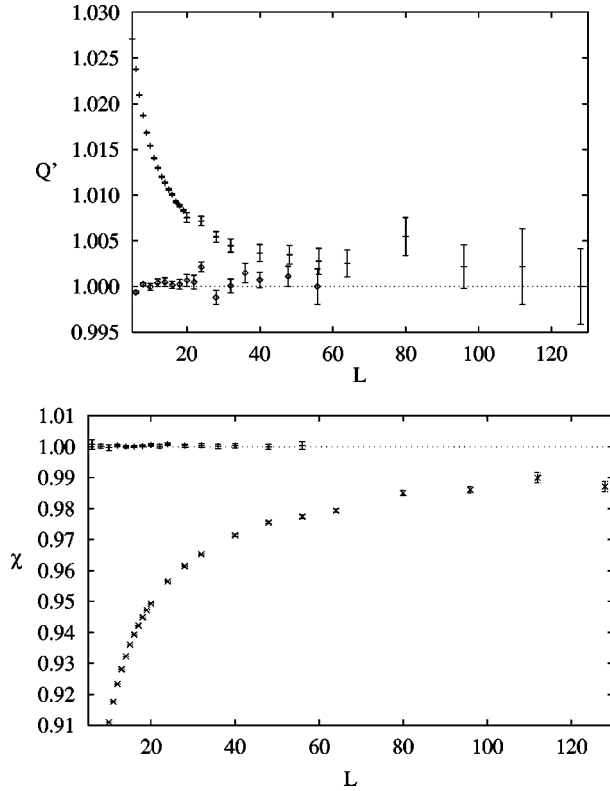


FIG. 3. Rescaled β derivatives of Q and rescaled χ at fixed Q as function of lattice size for both models (see text).

improvement in the scaling behavior that we demonstrated with our plots does not lead to reduced errors in final results for critical exponents. Taking the data of the improved model by itself they are in fact right. Since the coupling parameters of the model are determined numerically one has to expect some small residual $L^{-\omega}$ corrections, which lead to systematic errors when not taken into account in the fit *Ansätze*.

However, we shall demonstrate that it is well possible to estimate the effects of residual corrections to scaling in a systematic way. We shall exploit the fact that ratios of correction to scaling amplitudes are universal. Given the parametrization

$$R_i(L) = R_i^* + r_i L^{-\omega} + \dots, \quad (23)$$

and

$$\frac{dR_i}{d\beta} = c_i L^{1/\nu} (1 + b_i L^{-\omega} + \dots), \quad (24)$$

the ratios r_i/r_j and b_i/r_j do not depend on the details of the models chosen.¹⁷ In particular, they are the same for the standard and improved action. These ratios can be obtained from the analysis of the standard Ising model data and then used in order to estimate the residual correction to scaling amplitudes in the improved action results.

A. R_2 at fixed R_1

Analyzing the standard model data, it turns out that the Binder cumulant Q evaluated at a fixed value of Z_a/Z_p is the optimal quantity to detect corrections to scaling. (Doing

finite-size scaling with quantities taken at β values where a phenomenological coupling is kept to a fixed value is inspired by Ref. 18.) Optimal here means that the relative statistical error of the leading correction to scaling amplitude is the smallest. We computed Q at $Z_a/Z_p = 0.5425$. This means that first the function $\beta(L)$ is determined, which gives for each lattice size L the value of β such that Z_a/Z_p equals 0.5425. Then Q is computed for these $\beta(L)$. In the following we use \bar{Q} to denote this quantity. In principle Z_a/Z_p could be fixed to any value. For practical reasons, however, it is preferable to take a good approximation of $(Z_a/Z_p)^*$. To leading order \bar{Q} should behave as

$$\bar{Q} = Q^* + rL^{-\omega} + \dots \quad (25)$$

We first fitted the data obtained with the improved action, using as input $\omega = 0.81$ from Ref. 12. The fits were done on a sequence of data sets obtained by discarding data with $L < L_{\min}$. We obtained $Q^* = 0.623\,69(12)$, $0.623\,62(14)$, $0.623\,71(16)$ and $r = 0.0040(11)$, $0.0047(13)$, $0.0036(16)$ for $L_{\min} = 8, 10$, and 12 , respectively. All fits have a χ^2/dof close to 1.

There is still a small amplitude for corrections to scaling visible. The value of D where the leading order corrections vanish exactly should be slightly larger than the one used in this study.

In order to quantify the improvement that is achieved we have to compare with the data from the standard Ising model. To obtain a consistent result for Q^* from small lattices we had to include a subleading correction to scaling term $r'L^{-2\omega}$ in the *Ansatz*.

We obtained $Q^* = 0.623\,26(12)$, $0.623\,43(14)$, $0.623\,29(18)$, $r = 0.1131(19)$, $0.1092(27)$, $0.1128(43)$ and $r' = 0.0825(67)$, $0.102(12)$, $0.081(24)$ for $L_{\min} = 8, 10$, and 12 , respectively. Starting from $L_{\min} = 8$ the fits have a small χ^2/dof . The result for Q^* obtained from $L_{\min} = 10$ is consistent with the results from the improved action. There is a clear signal for the leading order corrections to scaling. The corresponding amplitude is stable when L_{\min} is varied. Also subleading corrections are well visible.

From the comparison of the two models we conclude that leading corrections to scaling in the improved model are reduced by a factor of about $0.11/0.004 = 28$. In order to compute systematic errors due to neglecting $L^{-\omega}$ corrections in the analysis of the data obtained from the improved model we assume (taking into account the statistical errors in the amplitudes) that the leading corrections to scaling are reduced at least by a factor of 22.

Using the universality of ratios of corrections to scaling amplitudes this reduction has to be the same for all quantities. Hence, we can take the correction amplitudes obtained from the standard action and divide it by 22 to obtain a bound on the leading order corrections that are to be expected in the case of the improved model.

B. Fitting R_1 and R_2

We first fitted the R_i in order to obtain estimates for the phenomenological couplings R_i^* , and, in addition, for the

TABLE II. Fitting R_1 with Eq. (26), fixing $\omega=0.81$.

L_{\min}	R_1^*	Standard action			χ^2/dof
		β_c	r_1		
10	0.54275(14){49}	0.22165446(16){21}	0.0347(10)	1.81	
14	0.54304(23){44}	0.22165431(19){15}*	0.0318(22)	1.88	
16	0.54334(26){27}*	0.22165417(18){11}	0.0281(26)	1.69	
20	0.54269(40){24}	0.22165443(21){7}	0.0369(50)	1.43	

critical coupling β_c . Here, and in the following, we use as an estimate of the leading correction to scaling exponent $\omega=0.81(2)$ from Ref. 12.

1. Standard action, fit R_i

In the case of the standard action we fitted our data with the *Ansatz*

$$R_i(L, \beta_{\text{MC}}) = R_i^* + \frac{dR_i}{d\beta}(L, \beta_{\text{MC}}) \Delta\beta + r_i L^{-\omega}. \quad (26)$$

In addition to a correction to scaling term of the form $r_i L^{-\omega}$, we included a term that (to first order) corrects for deviations from criticality. $\Delta\beta$ is the difference between the critical β_c and $\beta=0.2216545$. Fitting R_1 to this law, we fixed $\omega=0.81$. The results for the fit parameters as function of L_{\min} are given in Table II. The procedure used to compute the estimates of the systematic errors (curly brackets) will be discussed later. In the table we mark with an asterisk the value of L_{\min} where the systematic error estimate becomes equal to or smaller than the statistical estimate.

The fits are reasonably stable. Redoing the fits with $\omega=0.78$ and $\omega=0.83$, we found that the dependence on the choice of ω is negligible compared to the statistical errors and the systematic errors quoted in Table II.

Next, we applied the same analysis to the cumulant R_2 . The correction to scaling amplitude of R_2 comes out considerably larger than that of R_1 , namely $r_2 \approx 0.1$. We made also fits with ω as free parameter. E.g., for $L_{\min}=8$ we obtain $\omega=0.980(9)$ with $\chi^2/\text{dof}=0.89$. This value of ω is significantly larger than 0.81, the latter value being presently ac-

cepted by us as a reliable estimate. It seems that the fit parameter compensates for the lack of subleading correction terms in the *ansatz*.

We also tried to fit R_1 and R_2 together (forcing them to take the same value of β_c and the same values for the exponents). For sake of simplicity we assumed in these fits that R_1 and R_2 are statistically uncorrelated. We used ω as a free parameter. For R_2 we added a subleading correction term $r'_2 L^{-x}$. We checked the two possibilities to either fix the exponent x to some value or subject it to fitting in order to assume some effective value. Indeed, beyond the leading correction to scaling exponent ω , there are several exponents that could enter the game, like for instance 2ω , $x \approx 2$, or $1/\nu + \omega$. In Table III we present the fit results.

Notice that the amplitude of the leading correction to scaling is much smaller for R_1 , as expected, and for R_2 also the amplitude of the next-to-leading correction to scaling r'_2 is significantly different from zero. The effective next-to-leading exponent is of order two, and actually compatible with that appearing in the improved case.

The errors of this fit are smaller than the (safer) errors obtained from the fits with fixed ω . However, as a consequence of the limited number of lattice sizes available, the fit with many parameters cannot be checked for stability with respect to varying L_{\min} .

Finally, we tried to estimate the systematic errors of the fits discussed in the first part of this section that are caused by missing subleading correction to scaling terms. For this purpose we used the results obtained above. Table III shows that the value of r'_2 does not depend strongly on x . The same holds for r'_1 , which is estimated to be of order 0.02 obtained from a four-parameter fit with $\omega=0.81$, $x=2.3$ fixed.

We fitted separately (as in the first part of this section) to Eq. (26) the quantities defined by

$$\tilde{R}_i(L) = R_i(L) - r'_i L^{-x}, \quad (27)$$

where $R_i(L)$ are the original (Monte Carlo) data, and r'_i and x have fixed values determined by the fits discussed above, namely $r'_1=0.02$, $r'_2=0.184$, and $x=2.3$. Roughly speaking,

TABLE III. Fitting together R_1 and R_2 for $L_{\min}=8$. For R_1 we used Eq. (26), while for R_2 also an effective next-to-leading correction $r'_2 L^{-x}$ was added.

x	Standard action			
	R_1^*	R_2^*	β_c	ω
1.62	0.54120(19)	0.62295(25)	0.22165516(11)	0.670(37)
2.0	0.54256(15)	0.62261(25)	0.22165443(11)	0.772(31)
2.4	0.54305(13)	0.62325(24)	0.22165437(11)	0.865(27)
2.30(41)	0.54285(31)	0.62261(29)	0.22165428(14)	0.800(58)
Final	0.54334(26){27}	0.62292(31){21}	0.22165431(19){15}	
x	r_1	r_2	r'_2	χ^2/dof
1.62	0.0324(20)	0.058(11)	0.168(19)	4.40
2.0	0.0330(19)	0.0907(87)	0.152(25)	1.60
2.4	0.0373(17)	0.1151(72)	0.136(36)	1.31
2.30(41)	0.0334(28)	0.100(32)	0.184(25)	1.63

TABLE IV. Fitting separately the R_i with Eq. (28). The numbers in square and curly brackets are estimates of the systematic errors (see text).

Improved action			
L_{\min}	R_1^*	β_c	χ^2/dof
8	0.54213(8)[24]{66}	0.3832470(8)[8]{36}	1.78
10	0.54240(10)[19]{32}	0.3832453(9)[5]{15}	0.79
12	0.54251(11)[17]{21}	0.3832447(9)[4]{9}*	0.49
16	0.54260(15)[16]{15}*	0.3832442(11)[4]{5}	0.46
20	0.54252(25)[13]{10}	0.3832446(14)[2]{3}	0.55

L_{\min}	R_2^*	β_c	χ^2/dof
8	0.62447(6)[76]{30}	0.3832499(10)[46]{29}	2.22
10	0.62429(7)[62]{15}	0.3832479(12)[31]{12}	1.39
12	0.62414(8)[57]{11}	0.3832465(11)[26]{9}	0.42
16	0.62405(12)[50]{7}	0.3832457(14)[20]{5}	0.31
20	0.62393(18)[43]{4}	0.3832447(18)[17]{3}*	0.28

the $\tilde{R}_i(L)$ are the original data after subtraction of an estimate of the subleading correction to scaling contamination.

The absolute values of the differences between the R_i^* and β_c obtained in this way and those obtained from fitting $R_i(L)$ with the same equation are the estimates of the systematic errors given (inside curly brackets) in Table II.

In summary, from Table II (and from fit results not presented in a table) we obtain the following final estimates (labeled with a * in the table)

$$R_1^* = 0.543\,34(26)\{27\},$$

$$\text{standard action: } R_2^* = 0.622\,92(31)\{21\}$$

$$\beta_c = 0.221\,654\,31(19)\{15\} \text{ from } R_1,$$

$$\beta_c = 0.221\,654\,05(23)\{25\} \text{ from } R_2.$$

2. Improved action, fit R_i

We fitted the data to

$$R_i(L, \beta_{\text{MC}}) = R_i^* + \frac{dR_i}{d\beta}(L, \beta_{\text{MC}}) \Delta\beta. \quad (28)$$

Again, we included a term which corrects for deviations from criticality. β_{MC} is our simulation coupling 0.383 245. The fit parameters are R_i^* and β_c , entering through $\Delta\beta = \beta_{\text{MC}} - \beta_c$. We first fitted separately R_1 and R_2 in order to compare their scaling behavior. The results are reported in Table IV.

For estimates obtained from the improved action we give, in addition to the usual error bars, for each fit parameter two systematic errors. They should be understood as estimates of the uncertainty due to corrections to scaling terms. The first one, in square brackets, estimates the error made neglecting a leading correction scaling term. The second one, in curly brackets, estimates the error induced by neglecting subleading corrections to scaling. The error estimates were obtained in a well defined way to be described below.

We also fitted all the R_i data together with three parameters (R_1^* , R_2^* , and β_c). The results are presented in Table V.

Let us look at the results from a simultaneous fit of R_1 and R_2 with the law

$$R_i(L, \beta_{\text{MC}}) = R_i^* + \frac{dR_i}{d\beta}(L, \beta_{\text{MC}}) \Delta\beta + r_i L^{-x}. \quad (29)$$

x represents an effective exponent. Enforcing $x = \omega = 0.81$, we observed that χ^2/dof is a little larger than for the other values of x . The correction amplitudes r_i are very small. The main problem of this fit is that the ratio r_1/r_2 is completely inconsistent with that found for the standard Ising action. Leaving x free, it tends to choose a value around 2.5. The results are consistent with those obtained from fits (with a larger L_{\min}) without corrections to scaling. The χ^2/dof values do not allow to discriminate between the different values of the exponent. Obtaining estimates from a (relatively) large lattice limit of fits without correction to scaling is, in this case, a safer procedure compared to a multiparameter fit on all lattice sizes.

Finally we estimate systematic errors due to neglecting the leading correction to scaling term as well as subleading correction to scaling terms. For the estimates of errors due to leading corrections to scaling we used the following procedure (analogously used also in the following sections). From Table II we know with good precision the leading correction amplitudes $r_i^{(S)}$ for the standard action. From the universality argument discussed in the introductory part of Sec. IV, we assume that the corresponding amplitudes for the improved action are given by $r_i^{(S)}/22$. We define the tilde quantities

$$\tilde{R}_i(L) = R_i(L) - \frac{r_i^{(S)}}{22} L^{-\omega}. \quad (30)$$

Fitting \tilde{R}_i and R_i with Eq. (28) and taking the absolute value of the differences of the outcome parameters gives the estimates reported in square brackets.

The information from the fits according to Eq. (29) with the extra exponent x is used (as in the previous section) to

TABLE V. Fitting simultaneously the R_i with Eq. (28).

Improved action				
L_{\min}	R_1^*	R_2^*	β_c	χ^2/dof
8	0.54206(7)[11]{65}	0.62441(5)[64]{32}	0.3832481(6)[13]{34}	2.19
10	0.54231(9)[7]{32}	0.62421(6)[51]{16}	0.3832463(7)[8]{14}	1.21
12	0.54245(11)[7]{22}	0.62408(7)[46]{11}	0.3832453(8)[6]{9}	0.51
16	0.54254(14)[6]{14}*	0.62399(8)[40]{7}	0.3832448(9)[6]{5}*	0.42
20	0.54252(22)[4]{9}	0.62393(13)[35]{5}	0.3832446(11)[4]{3}	0.41

TABLE VI. Fitting $dR_1/d\beta$ (top) and $dR_2/d\beta$ (bottom) with Eq. (32).

Standard action			
L_{\min}	a_1	ν	χ^2/dof
10	-1.4723(7)	0.62981(7)[102]	5.38
20	-1.4798(26)	0.63045(21)[85]	1.00
28	-1.4747(36)	0.63008(27)[69]	0.88
40	-1.4757(79)	0.63014(54)[55]*	0.96
48	-1.4699(13)	0.62977(88)[48]	1.09
Standard action			
L_{\min}	a_2	ν	χ^2/dof
14	0.87050(71)	0.6331(1)[31]	3.35
24	0.8592(29)	0.6315(4)[18]	0.66
40	0.8501(76)	0.6305(9)[13]	0.26
48	0.850(12)	0.6304(13)[11]*	0.31
56	0.848(14)	0.6303(15)[11]	0.39

estimate in a systematic way the effect of ignoring the corresponding corrections. We define

$$\tilde{R}_i(L) = R_i(L) - r_i L^{-x}, \quad (31)$$

where x and r_i are parameters obtained by fitting with Eq. (29), namely $r_1 = -0.15$, $r_2 = 0.07$, and $x = 2.46$. Repeating the steps followed above, one obtains the estimates given in curly brackets.

Using the fit estimates marked with an asterisk, i.e., where statistical and systematic error estimates are of the same order, we obtain our final estimates

$$\begin{aligned} R_1^* &= 0.542\,54(14)[6]\{14\} \\ \text{improved action: } R_2^* &= 0.623\,93(13)[35]\{5\} \\ \beta_c &= 0.383\,244\,8(9)[6]\{5\}. \end{aligned}$$

C. Fitting the derivatives of the R_i

1. Standard action, fit $dR_i/d\beta$

We first fitted the $dR_i/d\beta$ without correction to scaling,

$$\frac{\partial R_i}{\partial \beta} = a_i L^{1/\nu}. \quad (32)$$

The corresponding results are summarized in Table VI. As expected, both quantities suffer from strong corrections to scaling. Let us first estimate the systematic error due to the leading correction. We made fits with the *ansatz*

$$\frac{\partial R_i}{\partial \beta} = a_i L^{1/\nu} (1 + b_i L^{-\omega}). \quad (33)$$

Then, we defined

$$\tilde{\frac{\partial R_i}{\partial \beta}} = \frac{\partial R_i}{\partial \beta} - a_i b_i L^{1/\nu - \omega}, \quad (34)$$

and finally we fitted the tilde quantities to Eq. (32), fixing $\omega = 0.81$. The differences in the ν exponents are given in the square brackets of Table VI. The leading amplitude corrections b_i can be found in Table VII.

TABLE VII. Fitting $dR_2/d\beta$ with Eq. (33) and fixed $\omega = 0.81$.

Standard action				
L_{\min}	a_2	ν	b_2	χ^2/dof
8	0.8418(20)	0.62999(25){93}<20>	0.1103(59)	0.48
10	0.8396(29)	0.62973(36){61}<17>	0.1181(95)	0.47
12	0.8395(36)	0.62973(43){46}<14>*	0.119(13)	0.52
14	0.8333(48)	0.62908(55){37}<16>	0.147(19)	0.35

The derivative of R_2 suffers from stronger systematic effects than the R_1 derivative. Therefore, we include the ω correction into the fit *ansatz* [namely, we fit with Eq. (33)] and compute the systematic error made neglecting further subleading corrections to scaling. The fit results are given in Table VII and in Fig. 4, where also the ν exponents obtained from the fit with Eq. (32) are reported for comparison.

In the table we have included as a third error bar (in $\langle \rangle$ brackets) estimates of the systematic effect from varying ω from 0.77 through 0.85. This covers a $2\text{-}\sigma$ interval around the ω value 0.81(2). Again, the systematic error estimates in curly brackets take into account the omission of next-to-leading corrections to scaling. We fitted with the *ansatz*

$$\frac{\partial R_i}{\partial \beta} = a_i L^{1/\nu} (1 + b_i L^{-\omega} + b'_i L^{-x}), \quad (35)$$

and defined the tilde quantities subtracting a contribution $a_2 b'_2 L^{1/\nu - 2}$, with an estimate $b'_2 = -0.1$.

We quote as our final estimates

$$\begin{aligned} \text{standard action: } \nu &= 0.630\,14(54)[55] \quad (\text{from Table VI}) \\ \nu &= 0.629\,73(43)\{46\}\langle 14 \rangle \quad (\text{from Table VII}). \end{aligned}$$

2. Improved action, fit $\partial R_i/\partial \beta$

We fitted our data for the derivatives of the R_i with respect to β , according to Eq. (32). The results are given in Table VIII. The ν estimates of this table are plotted in Fig. 5.

Obviously, the derivatives of the cumulant scale better than those of Z_a/Z_p : while the cumulant's derivative gives a small χ^2/dof already for $L_{\min} = 6$, for the R_1 's derivative one needs $L_{\min} = 18$ in order to have a small χ^2/dof and to reach

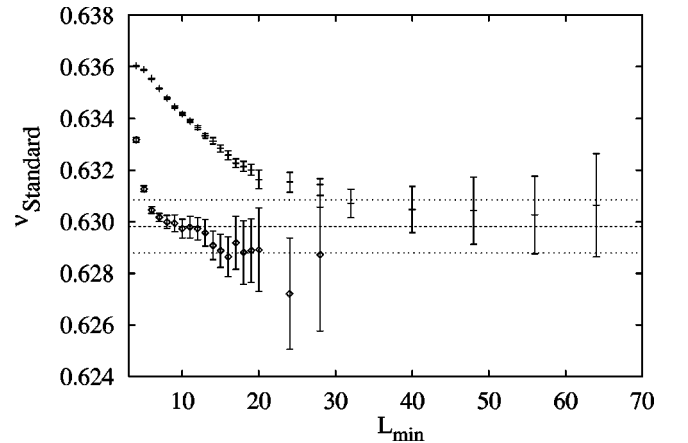


FIG. 4. ν resulting from fitting $dR_2/d\beta$, standard action, without correction to scaling (bars) and with $\omega = 0.81$ (diamonds).

TABLE VIII. Fit of $\partial R_1/\partial\beta$ (top) and $\partial R_2/\partial\beta$ (bottom) with Eq. (32).

Improved action			
L_{\min}	a_1	ν	χ^2/dof
10	-1.1419(12)	0.62850(14)[32]{152}	3.08
16	-1.1487(23)	0.62924(25)[27]{74}	0.90
20	-1.1543(39)	0.62979(39)[26]{43}	0.32
24	-1.1552(51)	0.62988(51)[32]{51}	0.40
L_{\min}	a_2	ν	χ^2/dof
6	0.66160(42)	0.62969(11)[22]{41}	0.79
8	0.66247(63)	0.62987(14)[18]{26}	0.57
10	0.6622(11)	0.62982(22)[16]{15}	0.60
12	0.6626(12)	0.62989(24)[24]{11}	0.64

stability of the result. However, also in this case the leading correction to scaling is strongly suppressed. Note that the range of lattice sizes considered here is relatively small: the difference in scaling behavior is actually due to a bigger amplitude of the next-to-leading correction to scaling, as discussed below.

The systematic error estimates due to neglecting leading order correction to scaling are given, as before, in square brackets. We defined tilde quantities by

$$\tilde{\partial R}_i = \frac{\partial R_i}{\partial\beta} - a_i \frac{b_i^{(S)}}{22} L^{1/\nu-0.81}, \quad (36)$$

where the a_i are given in Table VIII and the leading correction amplitudes $b_i^{(S)}$ of the standard action are taken from Table VII. The error estimates are the absolute differences of the ν 's obtained by fitting the tilde and the original Monte Carlo data, respectively, to Eq. (32).

The systematic error estimates due to subleading corrections are given in curly brackets.

To estimate them, we used a fit *ansatz*

$$\frac{\partial R_i}{\partial\beta} = a_i L^{1/\nu} (1 + b_i L^{-x}), \quad (37)$$

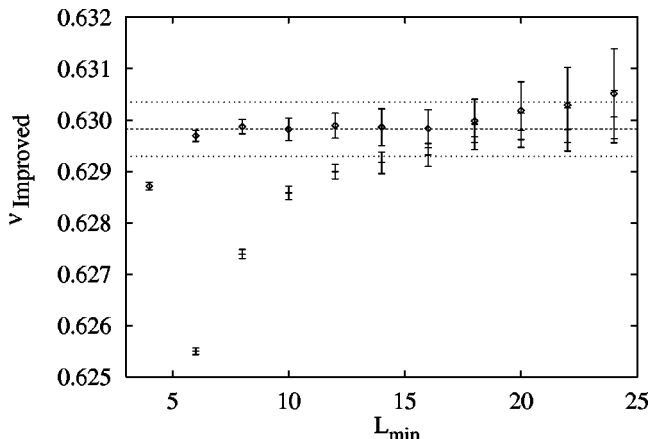


FIG. 5. Fit results for ν from fitting $\partial R_i/\partial\beta$, improved action, with Eq. (32). The data with better scaling behavior belong to $\partial R_2/\partial\beta$.

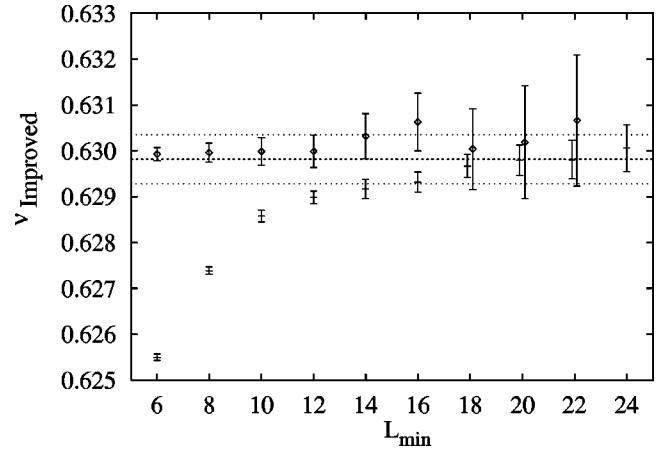


FIG. 6. Fits of $\partial R_1/\partial\beta$, improved action, with Eq. (32) (bars) and with Eq. (37) and $x=2.4$ fixed (diamonds).

and then defined the tilde quantities by subtracting $a_i b_i L^{1/\nu-2}$ from the Monte Carlo data.

We observed that including very small lattice sizes, the R_1 derivative's deviations from Eq. (32) are strong enough to allow for a fit with a free effective exponent, which turns out to be 2.33(28), i.e., again of order 2. Again we find that enforcing $x=0.81$ does not prevent the fit from giving an acceptable χ^2 . We have to rely on the universality of the ratios of correction amplitudes, as discussed before, to rule out this fit.

In Fig. 6 we plot the fits of $\partial R_1/\partial\beta$ using Eq. (37) for various values of L_{\min} with fixed exponent $x=2.4$, together with the fits without correction to scaling of Table VIII. This is sufficient to demonstrate the nice scaling behavior of the derivative of R_1 once an effective next-to-leading correction to scaling exponent of order 2 has been included in the fit.

In the case of $\partial R_2/\partial\beta$ the corrections are too small to allow for a free effective exponent fit. Therefore we fix the x values between 2.0 and 2.8, as suggested by the fits on $\partial R_1/\partial\beta$. The ν results are nicely stable within these bounds and consistent with the values obtained without scaling corrections.

These fits show clearly that the better scaling behavior of the Binder cumulant derivative is due to a smaller amplitude of the next-to-leading corrections to scaling compared to that of the Z_a/Z_p derivative.

Finally, we checked also for the systematic dependence on the location of β_c for R_2' , which is giving the most accurate result. We repeated the fits for the Q derivative on data from five shifted β values ranging from 0.383 243 to 0.383 247 in steps of 0.000 001, covering thus two standard deviations around our β_c estimate. The effect of this variation is negligible compared with the errors of Table VIII.

We thus quote as our final estimate for ν

$$\begin{aligned} \text{improved action: } \nu &= 0.62988(51)[32]\{51\} \text{ from } \partial R_1/\partial\beta, \\ \nu &= 0.62982(22)[16]\{15\} \text{ from } \partial R_2/\partial\beta. \end{aligned}$$

The final estimate of ν appears with dotted error lines in Figs. 5 and 6. The statistical and systematic errors were added up.

D. Fitting the susceptibility

The magnetic susceptibility is defined through

$$\chi = L^3 \langle m^2 \rangle, \quad (38)$$

with m being the normalized magnetization.

1. Standard action, fit χ

It turns out that the estimate of η from fits of the susceptibility χ taken at β_c depends quite strongly on the value of β_c . Taking the susceptibility at a fixed value of a phenomenological coupling removes this problem, as discussed in Ref. 18. One defines a function $\beta(L)$ by requiring that for any L the relation $R_i[L, \beta(L)] = \text{const}$ holds. The susceptibility is then computed at $\beta(L)$. We performed this analysis for the two cases of fixing $Q=0.6240$ and fixing $Z_a/Z_p=0.5425$. Note that in principle any value for Q and Z_a/Z_p that can be taken by the phenomenological couplings would work. However, for practical purposes it is the best to take good approximations of R_i^* .

We fitted our data to the *ansatz*

$$\chi[L, \beta_c(L)] = c + dL^{2-\eta}(1 + fL^{-\omega}), \quad (39)$$

where c is the leading analytic part of χ , and $fL^{-\omega}$ gives leading order corrections. In both cases an acceptable χ^2/dof is reached at $L_{\min}=10$. For $L_{\min}=10$ we obtained $c = -0.515(83)$, $d = 1.5600(44)$, $\eta = 0.03751(62)$, and $f = -0.585(12)$ with $Q=0.6240$ fixed and $c = -0.78(14)$, $d = 1.553(6)$, $\eta = 0.0366(8)$, and $f = -0.130(19)$ with $Z_a/Z_p=0.5425$ fixed.

It is interesting to see that the correction to scaling amplitude f is considerably smaller in the case of fixed Z_a/Z_p . Therefore it seems reasonable to assume that also $L^{-2\omega}$ corrections are smaller for fixed Z_a/Z_p . We thus take η from fixed Z_a/Z_p at $L_{\min}=10$ as our final result. As estimate of the systematic error we quote the difference to the fixed Q result at $L_{\min}=10$

$$\text{standard action: } \eta = 0.0366(8)\{9\}.$$

We have checked that the uncertainty in the estimate of ω leads to negligible errors in η . We also performed fits of the magnetic susceptibility without a constant term in the *ansatz*. It is reassuring that the results for η are consistent with those found above, when $L_{\min}=20$ is taken.

2. Improved action, fit χ

Also in the case of the improved action we computed the magnetic susceptibility at fixed $Q=0.6240$ and at fixed $Z_a/Z_p=0.5425$. We fitted our data with the *ansatz*

$$\chi[L, \beta(L)] = c + dL^{2-\eta}. \quad (40)$$

Here, we have skipped the term $L^{-\omega}$.

From the Ising model with the standard action we know that the amplitude of the $L^{-\omega}$ correction is much smaller for χ at fixed Z_a/Z_p than at fixed Q (see below). Therefore, the comparison of both results gives a nice check of the systematic errors introduced by the omission of a $L^{-\omega}$ term in the

fit *ansatz*. Since the corrections are smaller in the case of fixed Z_a/Z_p , we quote the corresponding result as our final estimate.

The systematic error due to the omission of a $L^{-\omega}$ term in the *ansatz* is computed in the same way as in the previous sections. Namely, we defined the tilde quantities as

$$\tilde{\chi}(L) = \chi(L) - d \frac{f^{(S)}}{22} L^{2-\eta-0.81}, \quad (41)$$

where $f^{(S)}$ are taken from the fits with Eq. (39). Then we compare the results obtained fitting the $\tilde{\chi}$ with Eq. (40) and the χ , both at fixed Q and fixed Z_a/Z_p . The absolute differences of the η obtained in this way are the estimates of the systematic errors. Notice that in this case the next-to-leading correction to scaling enters with an exponent of order 2, which is already taken into account with the analytical contribution denoted by c in our fit *Ansätze*. Therefore, we only quote the systematic error due to the leading correction.

We have chosen the result of $L_{\min}=8c = -0.532(62)$, $d = 0.9543(20)$, and $\eta = 0.03657(60)$ with $Z_a/Z_p=0.5425$ fixed as our final estimate, since it is consistent with the result obtained from $L_{\min}=4$ and $L_{\min}=6$. Hence, our final estimate is

$$\text{improved action: } \eta = 0.0366(6)[2].$$

It is consistent with the estimate obtained from the standard action.

V. COMPARISON WITH OTHER ESTIMATES

It is interesting to compare our estimates with other ones available from the literature. Note that extensive tables with many data from literature and experiment can be found in Refs. 8, 12, and 19.

Some of the more recent estimates for the ν and η exponents, together with the critical coupling of the standard Ising model are collected in Table IX. Our estimates are given in the last two lines: the upper one gives the estimates obtained with the standard action (SA) while the lower one those from the improved spin-1 action (IA). The underlined estimates are obtained by choosing our best estimate from the improved action and adding the statistical and systematic error estimates in order to obtain the overall uncertainty.

The value we obtained for the Binder cumulant from the improved action $Q = 0.62393(13)[35]\{5\}$ can be compared with the estimate $Q = 0.6233(4)$ of Ref. 8. It is reassuring that the high-precision estimates of the recent years seem to be nicely consistent with each other.

VI. CONCLUSIONS

By performing a detailed comparison with high-precision results of the standard action, we have demonstrated that the spin-1 Ising model with suitably tuned coupling constants has remarkably improved finite-size scaling properties. We obtained estimates of very high precision for the critical exponents ν and η and two other universal quantities, the Binder cumulant Q and the ratio of partition functions Z_a/Z_p .

All estimates from the two different actions are consistent

TABLE IX. Results of the present study from standard (SA) and improved (IA) actions are compared with other estimates: from ϵ expansion (EPS), field-theory calculations in three dimensions (3D FT), high-temperature expansions (HT), and Monte Carlo simulations (MC). The underlined estimates for the critical exponents are our best estimates together with error estimates, which give the overall uncertainty, including systematic effects.

Ref.	Method	ν	η	β_c
12	EPS	0.6293(26)	0.036(6)	
12	3D FT	0.6304(13)	0.0335(25)	
20	3D FT	0.6301(5)	0.0355(9)	
19	HT	0.6310(5)		
21	MC	0.6308(10)		
8 and 11	MC	0.6301(8)	0.037(3)	0.2216544(3)[3]
9	MC	0.6294(5)[5]	0.0374(6)[6]	0.22165456(15)[5]
SA	MC, R'_1	0.63014(54){55}		0.22165431(19){15}
SA	MC, R'_2	0.62973(43){46}{14}		0.22165405(23){25}
SA	MC, χ		0.0366(8){9}	
IA	MC, R'_2	0.62982(22)[16]{15}		
IA	MC, R'_2	<u>0.6298(5)</u>		
IA	MC, R'_1	0.62988(51)[32]{51}		
IA	MC, χ		0.0366(6)[2]	
IA	MC, χ		<u>0.0366(8)</u>	

with each other. In spite of the higher statistics and the bigger lattice sizes of the standard action data, the estimates from the improved action are by far more precise. In particular, cf. Table IX, the systematic errors are smaller for the improved action than for the standard action.

The authors of Refs. 9 and 10 claim that an improvement of the action as discussed in this paper and in Ref. 10 does not allow for more precise estimates of universal quantities such as the critical exponents. In their argument they ignore the fact that ratios of correction amplitudes are universal. Once these ratios are computed for the standard Ising model, where the corrections are large, they allow for powerful bounds in the case of the improved action. E.g., leading order corrections to scaling of the Binder cumulant are much stronger than those of the derivative of the Binder cumulant. Therefore it is quite clear that we can safely ignore $L^{-\omega}$ corrections in the analysis of Q' obtained from the improved model.

It would be worthwhile to use the present model in studies

of physical quantities not discussed in this paper and to check to what extent the improved scaling behavior helps to get better estimates.

An interesting question is whether and to what extent the improvement that we have achieved can be further enhanced. It seems tempting to study models with even more couplings in order to systematically reduce the effects from next-to-leading corrections to scaling. However, little is known about these higher order corrections, and one does not really know how many parameters would be necessary to remove corrections of order L^{-x} , with $x \approx 2$. Note that at that level of improvement also the question of improved observables comes into play. We thus believe that the improvement with two parameters, which we performed is the optimal thing one can do in a systematic way. Note that our improvement also eliminates subleading corrections of the type $L^{-n\omega}$.

Last but not least, application of the ideas underlying the present analysis to other models seems very promising.

*Electronic address: hasenbus@physik.hu-berlin.de

†Electronic address: pinn@uni-muenster.de

‡Electronic address: vinti@uni-muenster.de

¹M. Hasenbusch, K. Pinn, and S. Vinti, hep-lat/9806012 (unpublished).

²V. Privman, in *Finite Size Scaling and Numerical Simulations of Statistical Systems*, edited by V. Privman (World Scientific, Singapore, 1990).

³K. G. Wilson and J. B. Kogut, Phys. Rep., Phys. Lett. **12C**, 75 (1974); K. G. Wilson, Rev. Mod. Phys. **47**, 773 (1975); *ibid.* **55**, 583 (1983).

⁴The first article on this issue is P. Hasenfratz and F. Niedermayer, Nucl. Phys. B **214**, 785 (1994). An up-to-date reference list can

be found in P. Hasenfratz, Prog. Theor. Phys. Suppl. **131**, 189 (1998).

⁵K. Symanzik, Nucl. Phys. B **226**, 187 (1987); **226**, 205 (1987).

⁶See, e.g., the various contributions to the *LATTICE 97 Symposium, Parallel Session Improvement and Renormalization* [Nucl. Phys. B (Proc. Suppl.) **63**, 847 (1998)].

⁷J.-H. Chen, M. E. Fisher, and B. G. Nickel, Phys. Rev. Lett. **48**, 630 (1982); M. Barma and M. E. Fisher, *ibid.* **53**, 1935 (1984); Phys. Rev. B **31**, 5954 (1985); M. E. Fisher and J.-H. Chen, J. Phys. (Paris) **46**, 1645 (1985).

⁸H. W. J. Blöte, E. Luijten, and J. R. Heringa, J. Phys. A **28**, 6289 (1995).

⁹H. G. Ballesteros, L. A. Fernández, V. Martín-Mayor, A. Muñoz

- Sudupe, G. Parisi, and J. J. Ruiz-Lorenzo, *J. Phys. A* **32**, 1 (1999).
- ¹⁰H. G. Ballesteros, L. A. Fernández, V. Martín-Mayor, and A. Muñoz Sudupe, *Phys. Lett. B* **441**, 330 (1998).
- ¹¹A. L. Talapov and H. W. J. Blöte, *J. Phys. A* **29**, 5727 (1996).
- ¹²R. Guida and J. Zinn-Justin, *J. Phys. A* **31**, 8103 (1998).
- ¹³M. Creutz, *Phys. Rev. Lett.* **50**, 1411 (1983).
- ¹⁴K. Rummukainen, *Nucl. Phys. B* **390**, 621 (1993).
- ¹⁵U. Wolff, *Phys. Lett. B* **228**, 379 (1989).
- ¹⁶M. Hasenbusch, *Physica A* **197**, 423 (1993).
- ¹⁷A. Aharony, P. C. Hohenberg, and V. Privman, in *Phase Transitions and Critical Phenomena*, edited by C. Domb and J. L. Lebowitz (Academic, New York, 1991), Vol. 14.
- ¹⁸H. G. Ballesteros, L. A. Fernández, V. Martín-Mayor, A. Muñoz Sudupe, G. Parisi, and J. J. Ruiz-Lorenzo, *Phys. Lett. B* **400**, 346 (1997).
- ¹⁹P. Butera and M. Comi, *Phys. Rev. B* **56**, 8212 (1997). An estimate for η may be obtained using $\gamma=1.2385(5)$ and the relation $\eta=2-\gamma/\nu$.
- ²⁰Results by Murray and Nickel, taken from Table 10 of Ref. 12. Errors from uncertainty of \tilde{g}^* are not taken into account.
- ²¹M. Hasenbusch and K. Pinn, *J. Phys. A* **31**, 6157 (1998). In this work, also $\alpha=0.1115(37)$ is obtained.